Evaluation of the Binary Interaction Energy Density between Styrene and Acrylonitrile Units and Its Temperature Dependence

Shixiong Zhu and Donald R. Paul*

Department of Chemical Engineering and Texas Materials Institute, The University of Texas at Austin, Austin, Texas 78712

Received June 21, 2001; Revised Manuscript Received November 6, 2001

ABSTRACT: The miscibility behavior in blends of monodisperse poly(styrene) (PS) of varying molecular weight and polydisperse styrene/acrylonitrile copolymers (SAN) of varying AN contents was studied at three different temperatures: 120, 200, and 250 °C. An accurate quantitative evaluation of the binary interaction energy density between S and AN, $B_{S/AN}$, was made at each temperature by analyzing the miscibility data using the copolymer/critical molecular weight method. The values of $B_{S/AN}$ determined by this powerful method show that the Flory−Huggins based interaction energy $B_{S/AN}$ decreases as temperature increases. An equation-of-state analysis using the Sanchez−Lacombe lattice fluid theory was performed to interpret the temperature dependence of $B_{S/AN}$. An empirical scheme was introduced to account for the temperature dependence of the Sanchez−Lacombe characteristic parameters for PS. With this modification the temperature dependence of the experimental $B_{S/AN}$ is well described by the Sanchez−Lacombe lattice fluid theory using a constant bare interaction energy $\Delta P^*_{S/AN}$.

Introduction

The thermodynamic interactions between polymer repeat units determine whether polymer blends are miscible or not and the nature of the interface and morphology when they are phase separated.[1] Consequently, accurately quantifying these energetic interactions is important for the design of multicomponent polymer blend systems and has received a lot of attention.[1]

A particularly important interaction is that between styrene (S) and acrylonitrile (AN) units in part because SAN copolymer forms the matrix of ABS materials which are often blended with other polymers. For example, one approach to improved heat resistance of ABS polymers is to blend the SAN with other polymers.[2,3] Because of the commercial importance of SAN, its phase behavior with other polymers has been extensively studied in recent years.[3−13] For example, Nishimoto et al. investigated blends of SAN copolymers with methyl methacrylate copolymers containing cyclohexyl methacrylate, phenyl methacrylate, and *tert*-butyl methacrylate.[13] Gan et al. examined blends of SAN copolymers with methyl methacrylate−glycidyl methacrylate copolymers.[14−16] Chu et al. studied blends of SAN with methyl methacrylate copolymers containing ethyl acrylate, *n*-butyl acrylate, and tribromostyrene.[17−19] Merfeld et al. investigated blends of SAN with styrene−pentabromobenzyl acrylate copolymers.[20] Aoki et al. examined the miscibility of SAN with polystyrene-*co*-(*N*-phenylmaleimide) and poly(styrene-*co*-maleic anhydride).[3] The phase behavior of blends of SAN copolymer with poly(α-methylstyrene-*co*-acrylonitrile) was studied by Gan et al.,[14] Aoki,[4] and Cowie et al.[2] For all these studies, quantification of the binary interaction energy density of the S/AN pair, or $B_{S/AN}$, was necessary. Unfortunately, the values of $B_{S/AN}$ reported by different research groups vary greatly (ranging from 4.99 to 8.14 cal/cm^3).[21] The objectives of this study are to provide a more exact value of $B_{S/AN}$ and to document and understand its temperature dependence.

One strategy to quantify the $B_{S/AN}$ is to observe the phase boundaries (molecular weight, copolymer composition, temperature) that separate miscible from immiscible regions for blends of SAN with other polymers or copolymers and interpret the results within the framework of an appropriate thermodynamic theory.[17−25] One of the disadvantages of this approach is that too many binary interaction energies must be extracted at the same time, for example, up to six parameters are required for copolymer−copolymer blends. Therefore, the resulting values may be compromised in accuracy because of compensation effects. An alternative and more accurate method used here is the so-called copolymer/critical molecular weight method,[18,19] described in the next section, which overcomes the drawbacks of the copolymer−copolymer phase mapping approach. Comparison of the measured temperature dependence of $B_{S/AN}$ with that predicted by modern theories will also be made.[26−29]

Copolymer/Critical Molecular Weight Method

The strategy used to obtain the binary interaction energy information requires the use of an appropriate thermodynamic theory of mixing. The Gibbs free energy of mixing per unit volume (Δg_{mix}) for a blend of monodisperse polymers A and B can be modeled by the Flory−Huggins theory,[30,31] i.e.

$$\Delta g_{mix} = B\phi_A\phi_B + RT\left[\frac{\rho_A\phi_A \ln \phi_A}{M_A} + \frac{\rho_B\phi_B \ln \phi_B}{M_B}\right] \quad (1)$$

where B is the binary interaction energy density, R is the universal gas constant, T is the absolute temperature, and ϕ_i, ρ_i, and M_i are the volume fraction, density, and molecular weight of component i, respectively. This equation combines a van Laar type heat of mixing with the combinatorial entropy of mixing. Hence, B includes the contributions of heat of mixing and other noncombinatorial effects. The last terms of eq 1 are always

* To whom correspondence should be addressed. E-mail: drp@che.utexas.edu.

10.1021/ma0110608 CCC: $22.00
Published on Web 02/16/2002

negative and, therefore, favor miscibility; their contribution can lead to miscibility when the component molecular weights are low enough even when the interaction energy density is unfavorable. The interaction energy density B is related to the Flory−Huggins interaction parameter χ by

$$B = \frac{\chi RT}{V_{\text{ref}}} \tag{2}$$

where V_{ref} is an arbitrary reference volume. The critical interaction energy at the boundary between miscibility and immiscibility, where the energy and entropy terms are balanced, is given by the following expression which represents an excellent approximation for most polydisperse polymers:[32−37]

$$B_{\text{critical}} = \frac{RT}{2}\left(\sqrt{\frac{\rho_{\text{A}}}{(\bar{M}_{\text{w}})_{\text{A}}}} + \sqrt{\frac{\rho_{\text{B}}}{(\bar{M}_{\text{w}})_{\text{B}}}}\right)^2 \tag{3}$$

where $(\bar{M}_{\text{w}})_i$ is the weight-average molecular weight of polymer i. The Flory−Huggins theory assumes the polymer mixture is incompressible, which inherently means B must depend on temperature. Equation-of-state (EOS) theories include compressibility and, thus, account for the temperature dependence arising from volumetric contributions; of course, other factors may contribute temperature dependence to the observed interaction energy. In this study, the lattice fluid (LF) theory developed by Sanchez and Lacombe is used due to its versatility and simplicity.[26−29,38]

The Sanchez−Lacombe equation-of-state is expressed in terms of reduced properties:

$$\tilde{\rho}^2 + \tilde{P} + \tilde{T}\left[\ln(1-\tilde{\rho}) + \left(1 - \frac{1}{r}\right)\tilde{\rho}\right] = 0 \tag{4}$$

where chain length $r = MP^*/kT^*\rho^* = M/v^*\rho^*$, $\tilde{P} = P/P^*$, $\tilde{T} = T/T^*$, and $\tilde{\rho} = 1/\tilde{v} = \rho/\rho^*$.

The variables with asterisks are characteristic parameters usually determined by fitting experimental PVT data for the homopolymers to eq 4 and applying mixing rules for copolymers. The characteristic pressure of the mixture P^* is related to the characteristic pressures of the components, P_i^*, and the bare interaction energy ΔP^* as follows:

$$P^* = \phi_1 P_1^* + \phi_2 P_2^* - \phi_1\phi_2\Delta P^* \tag{5}$$

In this study, the binary interaction model is employed to quantitatively represent the polymer−polymer interactions;[39−41] it accounts quite well for the multiple intramolecular and intermolecular interactions that contribute to the net interaction energy density in eq 1. In this model, the net interaction energy density B is expressed in terms of the interactions between the various pairs of monomer units, B_{ij}, present and their volume fraction, ϕ_i, in the copolymer. For a blend of homopolymer PS and copolymer SAN, this model can be simplified to the following:

$$B = B_{\text{S/AN}}\phi_{\text{AN}}^{\ 2} \tag{6}$$

where ϕ_{AN} is the volume fraction of AN in the SAN copolymer.

The copolymer/critical molecular weight method combines the so-called critical molecular weight method with copolymer composition mapping.[17−19,32,40,42−44] The equation that describes the boundary between miscibility and immiscibility at a given temperature is obtained by combining eqs 3 and 6, i.e.,

$$\phi_{\text{AN}} = \sqrt{\frac{B_{\text{critical}}}{B_{\text{S/AN}}}} \tag{7}$$

Thus, a plot of ϕ_{AN} vs $\sqrt{B_{\text{critical}}}$ leads to a diagram where miscible blends are separated from the immiscible blends by a straight line passing through the origin with a slope of $1/\sqrt{B_{\text{AN}}}$. As can be seen, this method is powerful since it allows the determination of one B_{ij} at a time and a straightforward analysis of error limits; more importantly, it is more accurate. However, it is useful only when a series of monodisperse homopolymers (comprised of monomer 1) of widely varying molecular weight are available for blending with a series of copolymers (monomers 1 and 2) of varying composition. Because of its accuracy and simplicity, this method has become a focus of our research as illustrated.[18,19] However, it should be noted that at very low molecular weights end groups can become an issue as we have noted previously.[32]

Experimental Section

Materials. The PS homopolymer standards and most of the SAN copolymers of different AN compositions used in this study are described elsewhere;[17−19] however, an additional SAN copolymer containing 5.5 wt % of AN ($\bar{M}_{\text{w}} = 212\,000$) is used here. The densities of the polymers were determined at 30 °C by a density gradient column.

Blend Preparation. Monodisperse homopolymers PS with various molecular weights were blended with SAN copolymers of different AN contents. Blends containing equal masses of PS and SAN were cast from dichloromethane solution at room temperature. These blends were then dried in a vacuum oven while increasing the temperature 20 °C every day until the designated annealing temperature was reached and thermodynamic equilibrium was further established. The three annealing temperatures used in this study are 120, 200, and 250 °C.

Special attention was paid at higher annealing temperatures, i.e., 200 and 250 °C, to issues of polymer stability. The AN segments in SAN copolymer with high AN content can undergo some degree of intramolecular cyclization reaction, causing the blends to become yellow as annealing time increases.[45−47] Therefore, the appropriate annealing time was determined by periodically checking whether the equilibrium state was established or not as annealing time was varied. The higher the annealing temperature, the shorter the annealing time needed since a blend can reach its equilibrium state faster the higher the temperature.

Blend Assessment. Glass transition temperatures were determined to assess blend miscibility with a Perkin-Elmer DSC-7 system at a scanning rate of 20 °C/min. A first scan was run up to the corresponding annealing temperature to erase the thermal history, and a second run was made for thermal analysis. Whenever the glass transition temperatures (T_{g}) of the two components of the blends were too close to each other, phase behavior was determined visually.

Results and Discussion

Results. Miscibility data for PS/SAN blends are plotted, in the manner suggested by eq 7, in Figure 1 for 120, 200, and 250 °C where open circles represent miscible blends and closed circles represent immiscible blends.

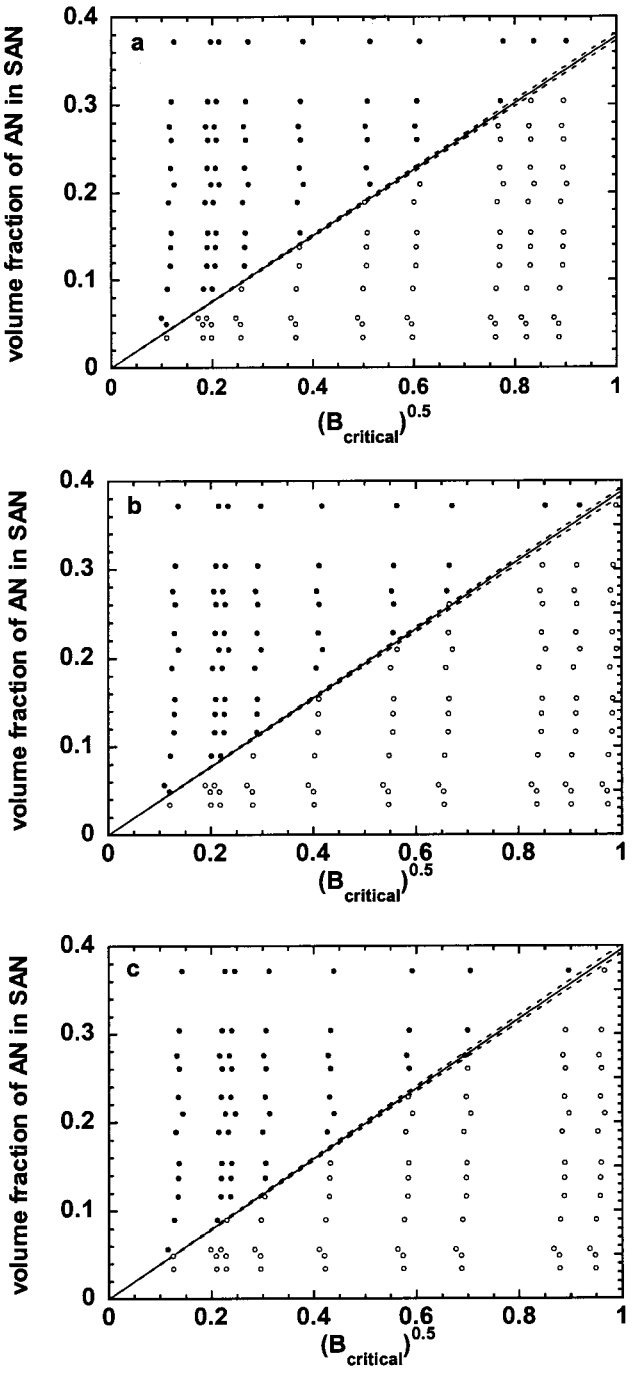

Figure 1. Isothermal miscibility maps at (a) 120, (b) 200, and (c) 250 °C for 50/50 blends of SAN copolymers with PS homopolymers of varying molecular weights plotted according to eq 7: (○) miscible; (●) immiscible. From the slopes of the lines separating the miscible and immiscible blends the following was calculated: $B_{S/AN} = 7.03 \pm 0.15$ cal/cm^3 at 120 °C, $B_{S/AN} = 6.65 \pm 0.16$ cal/cm^3 at 200 °C, and $B_{S/AN} = 6.35 \pm 0.16$ cal/cm^3 at 250 °C.

At 120 °C, for the SAN containing 3.8 wt % AN, all blends are miscible regardless of the molecular weight of the monodiperse PS. The blends containing the highest molecular weight (100 000 g/mol) PS became immiscible with SAN copolymers at 5.5 wt % and above AN. The blends of the lowest molecular weight (580 g/mol) PS did not become immiscible until the AN content was below 40 wt %. At 200 °C, more blends were observed to be miscible. When the annealing temperature was raised to 250 °C, even more blends were miscible than at 200 °C.

Table 1. Sanchez−Lacombe Characteristic Parameters Used in This Study

polymer	T^* (K)	P^* (MPa)	ρ^* (g/cm^3)	temp (°C)	std dev of specific vol (cm^3/g)	reference
PS	746	396	1.115	115−195	8.78×10^{-4}	this study
PS	754	399	1.1124	150−200	8.3×10^{-4}	this study
PS	807	373	1.0931	220−270	7.06×10^{-4}	this study
PAN	853	535.7	1.2299	150−200		50

In these plots of ϕ_{AN} vs $\sqrt{B_{critical}}$, a straight line passing through the origin can be drawn that well separates the miscible from the immiscible blends (see the solid lines in Figure 1). The error limits can be estimated by constructing the dashed lines shown. The values of $B_{S/AN}$ determined from the slopes of the various lines shown are 7.03 ± 0.15 cal/cm^3 at 120 °C, 6.65 ± 0.16 cal/cm^3 at 200 °C, and 6.35 ± 0.16 cal/cm^3 at 250 °C.

The interaction parameters in the Flory−Huggins framework B can be translated into that of the lattice fluid framework ΔP^* and vice versa by the following:[48,49]

$$B = \tilde{\rho}\Delta P^* + \left\{[P_2^* - P_1^* + (\phi_2 - \phi_1)\Delta P^*] + \frac{RT}{\tilde{\rho}}\left(\frac{1}{r_1^0 v_1^*} - \frac{1}{r_2^0 v_2^*}\right) - RT\left(\frac{\ln(1-\tilde{\rho})}{\tilde{\rho}^2} + \frac{1}{\tilde{\rho}}\right)\left(\frac{1}{v_1^*} - \frac{1}{v_2^*}\right)\right\}^2 \Big/ \left\{\frac{2RT}{v^*}\left[\frac{2\ln(1-\tilde{\rho})}{\tilde{\rho}^3} + \frac{1}{\tilde{\rho}^2(1-\tilde{\rho})} + \frac{1-1/r}{\tilde{\rho}^2}\right]\right\} \quad (8)$$

For accuracy purposes, the characteristic parameters, P^*, T^*, and ρ^* used in the above calculations for PS were recomputed from *PVT* data published previously.[50] It has been noted previously that better fits of the LF equation-of-state to experimental *PVT* data can be obtained by use of limited temperature ranges;[15,25,38,48,50,51] this seems especially so for polystyrene. The refitted characteristic parameters and the corresponding standard deviations in terms of specific volume for three temperature ranges are listed in Table 1. It should be noted that the parameters obtained here lead to lower standard deviations than by the previously reported fitting procedure.[50] Because of the inadequacy of *PVT* data available for every SAN copolymer, characteristic parameters for PAN published previously (see Table 1) will be used to calculate these values for SAN using approximate mixing rules.[50]

Figure 2 shows the experimentally determined values of $B_{S/AN}$ plotted vs temperature. The three solid curves were calculated from eq 8 using the characteristic parameters found in Table 1 in the following way. The PS characteristic parameters for the temperature range of 115−195 °C were used to determine a value of $\Delta P^*_{S/AN} = 7.35$ cal/cm^3 from the $B_{S/AN}$ determined at 120 °C. Likewise, the PS parameters for the temperature range of 150−200 °C were used to calculate a $\Delta P^*_{S/AN} = 7.22$ cal/cm^3 from the $B_{S/AN}$ determined at 200 °C while the temperature range of 220−270 °C was used to obtain $\Delta P^*_{S/AN} = 7.21$ cal/cm^3 at 250 °C. It can be clearly seen that the Flory−Huggins-based interaction energy $B_{S/AN}$ decreases as temperature increases as expected from the literature.[17] On the other hand, the temperature dependence of $B_{S/AN}$ does not seem to be

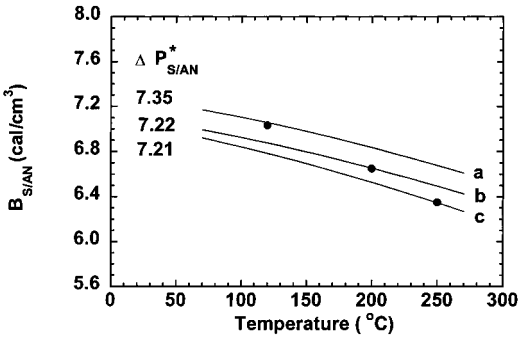

Figure 2. Effect of temperature on $B_{S/AN}$ values obtained from Figure 1. The solid curves were calculated according to eq 8 for the value of $\Delta P^*_{S/AN}$ shown using characteristic parameters calculated directly from experimental data for the temperature range: 150−200 °C for PAN and (a) 115−195, (b) 150−200, and (c) 220−270 °C for PS.

well described by the Sanchez−Lacombe theory with a constant $\Delta P^*_{S/AN}$, at least as determined by the method outlined using the three specific temperature ranges. The next section looks at this issue more carefully.

Equation-of-State Analysis. Some prior literature suggests that the temperature dependence of the Flory−Huggins-based interaction energies stems from equation-of-state effects,[48,50,51] at least when strong specific interaction are not involved, and can be well predicted by the Sanchez−Lacombe theory with a constant bare interaction energy ΔP^*. Chu and Paul considered the temperature dependence of the binary interaction energy values for the S/AN, MMA/AN, and S/MMA pairs over a wide temperature range using data from various sources.[17] They pointed out that the temperature range over which the equation-of-state parameters are evaluated can have an important effect on the predicted temperature dependence of the Flory−Huggins interaction energy. Furthermore, they noted for a given ΔP^*_{ij} the first term in eq 8 decreases with temperature, whereas the remaining group of terms generally increase with temperature. For large values of bare interaction energy ΔP^*, the second term only accounts for a small part of the total contribution. However, for small values of ΔP^*, the second term may be dominant and subtle changes in the characteristic parameters could strongly affect the trend with temperature.

It is now clear that two issues must be addressed more fully to reach a better understanding of the predicted temperature dependence of the Flory−Huggins interaction energy. First, most of the B values used to interpret the temperature dependence of B were obtained by copolymer−copolymer composition phase mapping and may not be accurate enough for such analysis. We believed that the current method is accurate enough for this purpose. Second, a better way is needed for dealing with the fact that the SL characteristic parameters depend on the temperature range of the PVT data from which they are extracted; sometimes this range does not correspond well to the temperature range of the phase behavior observations. We propose to deal with the second issue associated with the temperature dependence of the characteristic parameters in the following way. Figure 3 shows the T^*, P^*, and ρ^* values for PS from Table 1 over the different temperature ranges plotted vs temperature. A straight line (see the dashed lines in Figure 3) is used to connect the median values of the three horizontal lines. The equations representing these lines are shown in Table 2. We propose that these empirical relations should give a better representation of the PVT data for PS by the Sanchez−Lacombe equation over the whole experimental temperature range (from 114 to 258 °C). The resulting calculated specific volume data for PS are plotted against the experimental specific volume in Figure 4; the standard deviation is found to be 6.46×10^{-4} cm^3/g, which is smaller than any of those in Table 1. In turn, this implies that these characteristic parameters would

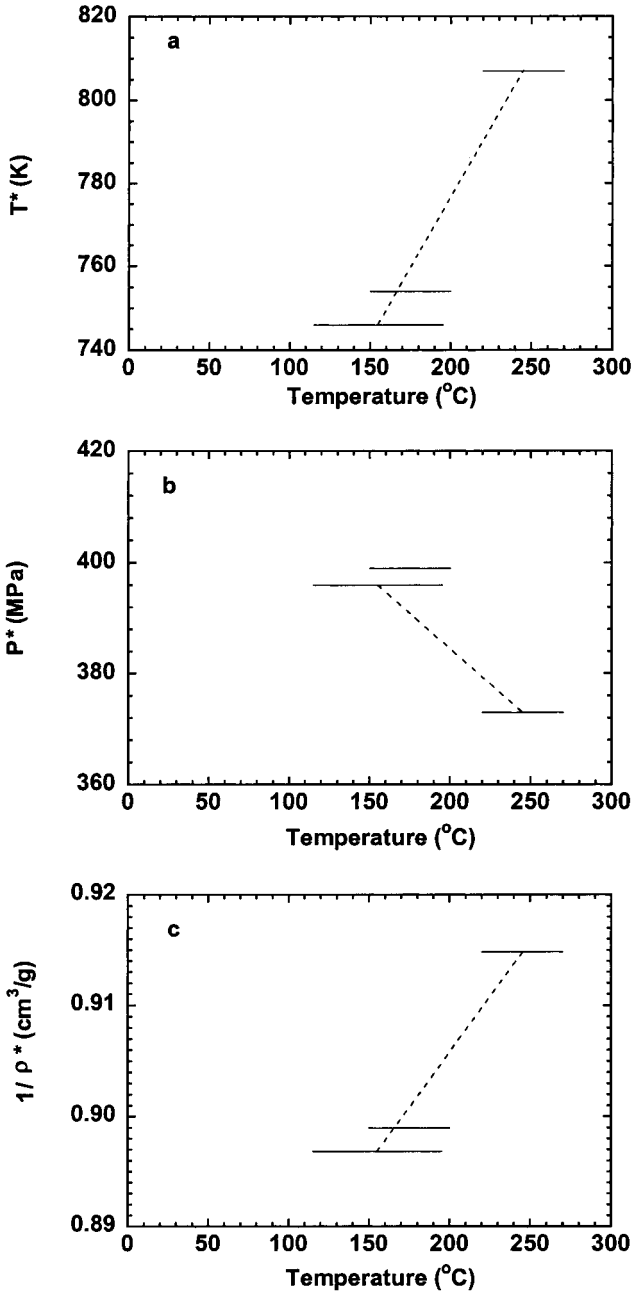

Figure 3. Sanchez−Lacombe characteristic parameters for PS as a function of temperature; The dashed lines were obtained by connecting the median values of the horizontal lines: (a) T^*; (b) P^*; (c) $1/\rho^*$.

Table 2. Equations for the Temperature-Dependent Characteristic Parameters; for These Equations, T Is in °C

polymer	T^* (K)	P^* (MPa)	$1/\rho^*$ (cm^3/g)
PS	$641.2 + 0.68T$	$435.6 - 0.26T$	$0.8660 + 0.0002T$
PMMA	$638.4 + 0.20T$	$464.6 + 0.086T$	$0.7775 + 3.61 \times 10^{-5}T$

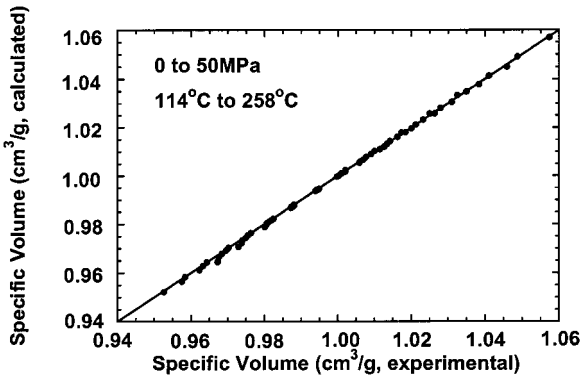

Figure 4. Calculated specific volume as a function of experimental specific volume for PS. The temperature-dependent characteristic parameters for PS listed in Table 2 were used in the calculation.

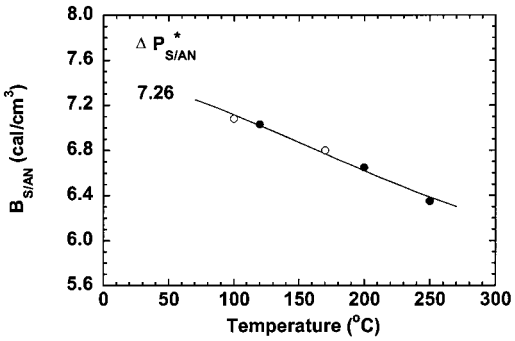

Figure 5. Effect of temperature on $B_{S/AN}$ values obtained from Figure 1 (●) and refs 14 and 15 (○). The solid curve was calculated according to eq 8 for the value of $\Delta P^*_{S/AN}$ shown using characteristic parameters listed in Table 2 for PS.

more correctly represent the thermodynamics of mixing and resulting predictions from eq 8 than the piecewise fitting used previously. Unfortunately, because of the instability and "crystalline" nature of polyacrylonitrile (PAN), no experimental *PVT* data are available for PAN homopolymer. Thus, a similar analysis cannot be made for PAN. The parameters for PAN shown in Table 1 were determined by fitting *PVT* for SAN copolymers and extrapolating the plots of the resulting characteristic parameters to 100% AN. A possible alternative approach for PAN is to fit data for the SAN copolymers over the whole temperature range using the procedure described for PS, then to plot the obtained slopes and intercepts vs AN content, and extrapolate to 100% AN. This effort has met with little success since the fitting parameters obtained for SAN copolymers does not show any simple relationship with AN content. As a result, we use the constant characteristic parameters for PAN in the following calculations. We propose that this is not a serious concern and that, in fact, the effect of temperature on SL characteristic parameters is more severe for PS than most other polymers. To test this proposal, plots similar to Figure 3 were made for PMMA,[38] and the resulting equations for the temperature-dependent characteristic parameters listed in Table 2 were deduced. As can be seen, the slopes for PMMA are much smaller than those for PS. Other polymers appear to be more similar to PMMA than PS.[38]

The line in Figure 5 shows the temperature dependence of $B_{S/AN}$ predicted from eq 8 using the equations for the characteristic parameters listed in Table 2 determined from Figure 3 for PS and those shown in Table 1 for PAN for a constant value of $\Delta P^*_{S/AN} = 7.26$ cal/cm^3. The solid line constructed by considering the temperature-dependent characteristic parameters for PS provides a very good description of the temperature dependence of $B_{S/AN}$. It should be noted that there are other experimental $B_{S/AN}$ values available at different temperatures from the literature.[21] However, some of these values are clearly not accurate; however, two experimental $B_{S/AN}$ values from the literature that are believed to be more accurate have been added to Figure 5.[14,15] Thus, it appears that to a good approximation $\Delta P^*_{S/AN}$ is independent of temperature.

Conclusion

The states of miscibility of blends of monodisperse PS homopolymers of varying molecular weight with polydisperse SAN copolymers of varying AN contents were determined at three different temperatures: 120, 200, and 250 °C. Analysis of these data using the copolymer/critical molecular weight method led to accurate binary interaction energies $B_{S/AN}$ at each temperature. An equation-of-state analysis was used to interpret the temperature dependence of $B_{S/AN}$. By an approximate treatment of the temperature dependence of the Sanchez−Lacombe characteristic parameters of PS, the temperature dependence of the experimental $B_{S/AN}$ is well-described by the Sanchez−Lacombe lattice fluid theory using a constant bare interaction energy $\Delta P^*_{S/AN}$.

Acknowledgment. This research was funded by National Science Foundation Grant DMR 97-26484 administered by the Division of Materials Research -Polymers Program.

References and Notes

(1) Paul, D. R., Bucknall, C. B., Eds.; *Polymer Blends: Formulation and Performance*; John Wiley & Sons Ltd.: New York, 2000; Vols. 1 and 2.
(2) Cowie, J. M. G.; Elexpuru, Elisa, M.; McEwen, I. J. *Polymer* **1992**, *33*, 1993.
(3) Aoki, Y. *Macromolecules* **1988**, *21*, 1277.
(4) Aoki, Y. *Macromolecules* **1988**, *21*, 6006.
(5) Callaghan, T. A. Ph.D. Dissertation, The University of Texas at Austin, 1992.
(6) Stein, D. J.; Jung, R. H.; Illers, K. H.; Hendus, H. *Angew. Makromol. Chem.* **1974**, *36*, 89.
(7) Chiou, J. S.; Paul, D. R.; Barlow, J. W. *Polymer* **1982**, *23*, 1543.
(8) Fowler, M. E.; Barlow, J. W.; Paul, D. R. *Polymer* **1987**, *28*, 1177.
(9) Lath, D.; Cowie, J. M. G.; Lathova, E. *Polym. Bull. (Berlin)* **1992**, *28*, 361.
(10) Suess, J.; Kressler, J.; Kammer, H. W. *Polymer* **1987**, *28*, 957.
(11) Kressler, J.; Kammer, H. W.; Klostermann, K. *Polym. Bull. (Berlin)* **1986**, *15*, 113.
(12) Nishimoto, M.; Keskkula, H.; Paul, D. R. *Polymer* **1989**, *30*, 1279.
(13) Nishimoto, M.; Keskkula, H.; Paul, D. R. *Macromolecules* **1990**, *23*, 3633.
(14) Gan, P. P.; Paul, D. R. *Polymer* **1994**, *35*, 3513.
(15) Gan, P. P. Ph.D. Dissertation, The University of Texas at Austin, 1994.
(16) Paul, D. R. *Pure Appl. Chem.* **1995**, *67*, 977.
(17) Chu, J. H.; Paul, D. R. *Polymer* **1999**, *40*, 2687.
(18) Chu, J. H.; Paul, D. R. *Polymer* **2000**, *41*, 5393.
(19) Chu, J. H.; Paul, D. R. *Polymer* **2000**, *41*, 7193.
(20) Merfeld, G. D.; Paul, D. R. *Polymer* **2000**, *41*, 663.
(21) Merfeld, G. D.; Paul, D. R. Polymer−Polymer Interactions Based on Mean Fileld Approximations. In *Polymer Blends: Formulation and Performance*; Paul, D. R., Bucknall, C. B., Eds.; John Wiley & Sons Ltd.: New York, 2000; Vols. 1 and 2, Chapter 3.
(22) Merfeld, G. D.; Paul, D. R. *Polymer* **1998**, *39*, 1999.

(23) Merfeld, G. D.; Paul, D. R. *J. Polym. Sci., Part B: Polym. Phys.* **1998**, *36*, 3115.
(24) Merfeld, G. D.; Chan, K.; Paul, D. R. *Macromolecules* **1999**, *32*, 429.
(25) Merfeld, G. D. Ph.D. Dissertation, The University of Texas at Austin, 1998.
(26) Sanchez, I. C.; Lacombe, R. H. *J. Phys. Chem.* **1976**, *80*, 2353.
(27) Sanchez, I. C.; Lacombe, R. H. *J. Polym. Sci., Polym. Lett.* **1977**, *15*, 71.
(28) Sanchez, I. C.; Lacombe, R. H. *Macromolecules* **1978**, *11*, 1145.
(29) Sanchez, I. C. Polymer Phase Separation. In *Encyclopedia of Physical Science and Technology*; Meyers, R. A., Ed.; Academic Press: New York, 1992; Vol. 13.
(30) Huggins, M. L. *J. Chem. Phys.* **1941**, *9*, 440.
(31) Flory, P. J. *J. Chem. Phys.* **1942**, *10*, 51.
(32) Callaghan, T. A.; Paul, D. R. *Macromolecules* **1993**, *28*, 2439.
(33) Koningsveld, R. *Br. Polym. J.* **1975**, *7*, 435.
(34) Koningsveld, R.; Chermin, H. A. G. *Proc. R. Soc. London, A* **1970**, *319*, 331.
(35) Koningsveld, R.; Kleintjens, L. A. *J. Polym. Sci., Polym. Symp.* **1977**, *61*, 221.
(36) Koningsveld, R.; Schoffeleers, H. M. *Pure Appl. Chem.* **1974**, *39*, 1.
(37) Salomons, W.; Brinke, G. T.; Karasz, F. E. *Polym. Commun.* **191**, *32*, 185.
(38) Sanchez, I. C.; Stone, M. T. Statistical Thermodynamics of Polymer Solutions and Blends. In *Polymer Blends: Formulation and Performance;* Paul, D. R., Bucknall, C. B., Eds.; John Wiley & Sons Ltd.: New York, 2000; Vols. 1 and 2, Chapter 2.
(39) Paul, D. R.; Barlow, J. W. *Polymer* **1984**, *25*, 487.
(40) Kambour, R. P.; Bendler, J. T.; Bopp, R. C. *Macromolecules* **1983**, *16*, 753.
(41) TenBrinke, G.; Oudhuis, L.; Ellis, T. S. *Thermochim. Acta* **1994**, *238*, 15.
(42) Takakuwa, K.; Gupta, S.; Paul, D. R. *J. Polym. Sci., Part B: Polym. Phys.* **1994**, *32*, 1719.
(43) Callaghan, T. A.; Paul, D. R. *J. Polym. Sci., Part B: Polym. Phys.* **1994**, *32*, 1813.
(44) Kambour, R. P.; Gundlach, P. E.; Wang, I. C. W.; White, D. W.; Yeager, G. N. *Polym. Commun.* **1988**, *29*, 170.
(45) Yabumoto, S.; Ishii, K.; Kawamori, M.; Arita, K.; Yano, H. *J. Polym. Sci., Polym. Chem. Ed.* **1969**, *7*, 1683.
(46) Johnson, J.; Potter, W.; Rose, P.; Scott, G. *Br. Polym. J.* **1972**, *4*, 527.
(47) Kressler, J.; Rudolf, B.; Shimomai, K.; Ougizawa, T.; Inoue, T. *Macromol. Rapid Commun.* **1995**, *16*, 631.
(48) Callaghan, T. A. Ph.D. Dissertation, The University of Texas at Austin, 1992.
(49) Kim, C. K.; Paul, D. R. *Polymer* **1992**, *33*, 1630.
(50) Kim, C. K. Ph.D. Dissertation, The University of Texas at Austin, 1993.
(51) Chu, J. H. Ph.D. Dissertation, The University of Texas at Austin, 1999.

MA0110608